

Superconducting Properties of Tin, Indium, and Mercury below 1° K*

D. K. FINNEMORE† AND D. E. MAPOTHER

Department of Physics, University of Illinois, Urbana, Illinois

(Received 3 May 1965)

The superconducting critical field curves for pure Sn, In, and Hg have been measured down to about 0.3°K. In the low-temperature region where the superconducting electronic entropy is negligible, the entropy difference (and hence the normal electronic entropy) is linear in temperature, as expected for a free electron gas. The measurements provide a sensitive test for details of the BCS theory in that the accuracy obtainable is much higher than in other experiments. A simple scaling of the energy-gap-to-temperature ratio brings the theoretical predictions into good agreement with experiment. The results are critically analyzed in the light of a possible lattice contribution to the entropy change at the superconducting transition of In, but no evidence for such a lattice contribution is found.

I. INTRODUCTION

THE entropy difference between the normal and superconducting states ($\Delta S = S_n - S_s$) is dominated by the contribution of the normal electrons as the temperature approaches 0°K. Values of ΔS can be directly calculated from measurements of the critical-field curve (H_c versus T). For H_c measurements extending to sufficiently low temperature the normal electronic entropy S_{en} may be separated and determined precisely. Since its original suggestion by Daunt and Mendelssohn,¹ this method has been applied in many investigations but, in most cases, it is questionable whether the range of temperature available was low enough to yield the true limiting behavior of ΔS as $T \rightarrow 0^\circ\text{K}$.

New critical field data are reported here for Sn, In, and Hg which have been extended to about 0.3°K using a He³ refrigerator. The results give reasonable verification that the temperatures achieved are indeed low enough to yield accurate values of the temperature coefficient of the normal electronic specific heat γ for all three elements. Since this determines the normal electronic-entropy contribution over the entire superconducting range, the experimental ΔS values may be analyzed to yield the complete temperature dependence of the superconducting electronic entropy. The results are examined from the standpoint of the Bardeen-Cooper-Schrieffer (BCS) theory.

II. EXPERIMENTAL PROCEDURE

The H_c data were obtained using the ballistic-induction technique which has been described in a previous article.² The only features not covered in earlier descriptions are those concerned with production and measurements of temperature below 1°K. The magnetic

measuring apparatus was designed around a He³ refrigerator which is similar in design and operation to units already described in the literature.³

A. Thermal Equilibrium

The inner chamber of the cryostat and all of its contents (Fig. 1) were designed to be in good thermal equilibrium. Two copper yokes maintained the transition pickup coils (E) in equilibrium with the He³ refrigerator; 32 equally spaced No. 20 copper wires (H) thermally linked the salt to the refrigerator. Adjacent cryostat surfaces which required good thermal contact were either soldered or coated with Apiezon J oil and clamped together. The refrigerator carbon resistor (G)

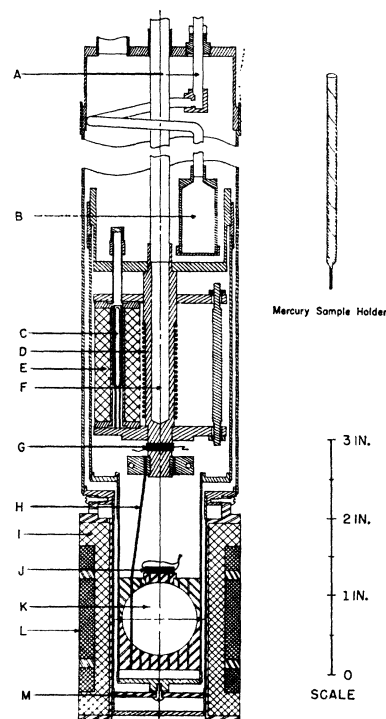


FIG. 1. Cross-section view of low-temperature section of cryostat. Refer to text for explanation of lettered items.

* Supported in part by the U. S. Office of Army Research (Durham).

† Present address: Department of Physics, Iowa State University, Ames, Iowa.

¹ J. G. Daunt and K. Mendelssohn, Proc. Roy. Soc. (London) **A160**, 127 (1937).

² J. F. Cochran, D. E. Mapother, and R. E. Mould, Phys. Rev. **103**, 1657 (1956).

³ K. W. Taconis, *Progress in Low Temperature Physics* (North-Holland Publishing Company, Amsterdam, 1961), Vol. III.

was cemented into its socket with Apiezon J oil; the salt-pill carbon resistor (J) was cemented to the salt pill and the copper wires (H) with Apiezon N. The N grease, in addition to providing thermal contact to the salt pill, sealed the salt from the air and thus inhibited the loss of water of hydration.

The superconducting specimens (C) could not be mechanically anchored to the cryostat because of the risk of strain which affects the superconducting behavior. Therefore, provision was made to admit 0.003 mole of He³ to the inner chamber. When good thermal contact was required between the inner chamber and the liquid He⁴ bath, 0.2 mole of He⁴ was admitted to the exchange-gas space.

From measurements of equilibrium times and heat leaks, an upper limit could be placed on thermal gradients between different parts of the cryostat. The only significant gradient was a possible 0.0006°K difference between the salt pill and the He³ refrigerator. Measurements of the critical field of Sn at 0.6°K showed no dependence of the critical field on the He⁴ bath temperature as the bath temperature was varied from 1.8 to 1.1°K.

B. Temperature Control and Measurement

Between 4.2°K and 1.1°K, isothermal conditions were maintained by controlling the pumping speed over a He⁴ bath and by controlling the power output of a heater located at the bottom of the bath consisting of an Allen Bradley 56 Ω, ½-W carbon resistor. Details of these methods have previously been published.² Below 1.1°K, isothermal conditions were maintained by controlling the pumping speed over a reservoir of He³ (F) and by controlling the power output of a noninductive heater (D) with a 470 Ω, ½-W Speer carbon resistor⁴ as the temperature-sensing element. Between 1.1 and 0.9°K, temperature was held constant within 0.001°K; below 0.9°K, it was held constant within 0.0005°K.

Above the λ point, temperature was determined from the vapor pressure of He⁴ condensed in a bulb (B) located in the exchange gas space. The 0.125-in. pressure-sensing line (A) was vacuum-jacketed from the top of the Dewar to the top of the outer can. Between the top of the outer can and the bulb, the tube spiraled outward and was soldered to the surface of the outer can to trap and absorb energy coming down the tube. The temperature difference between the bulb and the bath was measured at each temperature and was found to be from 1 to 7 millidegrees greater than the difference predicted from the head correction.⁵

Between the λ point and 1.1°K, temperature could not be reliably determined from the bulb measurements because there was a significant temperature drop (up

to 10 mdeg) across the Kapitza boundary resistance⁶ between the bulb surface and the He⁴. Both refluxing⁷ of He⁴ and conduction down the measuring tube are important factors in contributing heat to this effect. Instead of using the vapor pressure over the bulb, temperature was determined by sampling the vapor pressure over the bath with a vacuum jacketed tube. The temperature of the lower end of the tube, needed for the thermomolecular correction,⁸ was measured using a carbon resistor and was always <4.0°K. By sliding the tube through a hose fitting at the top of the Dewar, pressure could be determined as a function of height above the bath level. The pressure drop between the surface of the liquid and a point eight inches above the surface was less than 0.002 mm Hg. Temperature was determined from the vapor pressure measurements using the 1958 He⁴ scale of temperatures.⁹

Below 1.1°K, temperature was determined from the mutual inductance of coils containing chrome methylamine alum. The primary coil (I) was wound on a Dilecto coil form as a sixth-order Garrett system¹⁰ to provide uniform field over the volume of the salt pill. The secondary coil (L) was wound directly on the primary in three parts, the main coil around the salt and two bucking coils away from the salt. The salt pill (K) was a mixture of chrome methylamine alum crystals (particle size less than ½ mm) and 50-centistoke silicone oil tamped into the nylon form to a salt density of 1.1 g/cm³. The copper wires (H) were etched to a diameter of about 0.020 in. over the part of the wire in contact with the salt; a copper bead was formed by melting the lower end of the wire to seal the salt pill against draining of the silicone oil. The mutual inductance of this system was measured to a precision of 1.0 μH using a ballistic Hartshorn Bridge. The room-temperature mutual inductances were calibrated under the conditions of the run to a precision of 0.3 μH using a Heydweiller Bridge.

Absolute temperature was determined from the susceptibility of the salt by the Hebb and Purcell¹¹ relations with the Onsager¹² correction for the local magnetic field. Experimental determinations of the entropy¹³ and specific heat¹⁴ of a powdered sample as a function of susceptibility have verified these theoretical predictions. Thus, to determine the Kelvin temperature from the measured susceptibility of the salt χ, a magnetic (or Curie law) temperature T* is

⁶ L. I. Challis, *Proceedings of the Seventh International Conference on Low Temperature Physics* (University of Toronto Press, Toronto, 1961).

⁷ S. G. Sydorik and T. R. Roberts, *Phys. Rev.* **118**, 901 (1960).

⁸ T. R. Roberts and S. G. Sydorik, *Phys. Rev.* **102**, 304 (1956).

⁹ F. G. Brickwedde, H. van Dijk, M. Durieux, J. R. Clement, and J. K. Logan, *J. Res. Natl. Bur. Std. (U.S.)* **64A**, 1 (1960).

¹⁰ M. W. Garrett, *J. Appl. Phys.* **22**, 1091 (1951).

¹¹ M. H. Hebb and E. M. Purcell, *J. Chem. Phys.* **5**, 338 (1937).

¹² L. Onsager, *J. Am. Chem. Soc.* **58**, 1486 (1936).

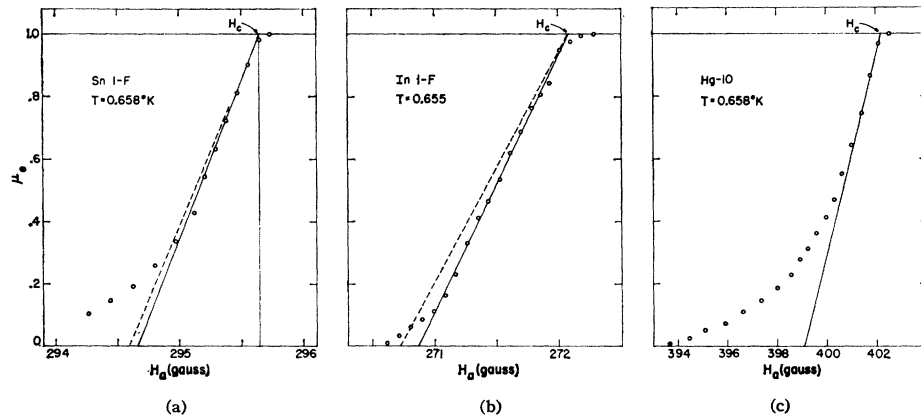
¹³ D. deKlerk and R. P. Hudson, *Phys. Rev.* **91**, 278 (1953).

¹⁴ W. E. Gardner and N. Kurti, *Proc. Phys. Soc. London* **A223**, 542 (1954).

⁴ W. C. Black, W. R. Roach, and J. C. Wheatley, *Rev. Sci. Instr.* **35**, 587 (1964).

⁵ F. E. Hoare and J. E. Zimmerman, *Rev. Sci. Instr.* **30**, 184 (1959).

FIG. 2. Typical magnetic transitions for (a) tin, (b) indium, and (c) mercury. The dashed lines where shown give the expected transition shape for an ideal ellipsoid having the same length-to-diameter ratio as the actual specimen.



defined by the equation

$$\chi = C/T^*,$$

where C is the Curie constant. The susceptibility of this salt does not follow Curie's law for two reasons: (a) The local magnetic field at the ions is not equal to the externally applied field, and (b) there is a crystalline electric field present in this salt. Applying the Onsager correction for the local magnetic field in a spherical sample gives

$$T^*_{\text{Ons}} = \frac{(T^* - 4\pi C/3V)(T^* + 8\pi C/3V)}{(T^* + 4\pi C/3V)}.$$

(T^*_{Ons} would be the Kelvin temperature if no other corrections had to be made.) Applying the Hebb and Purcell correction for the electric field splitting of the energy levels of the Cr^{3+} ions gives

$$T = T^*_{\text{Ons}} \frac{(3 + 4T/\delta) + (3 - 4T/\delta)e^{-\delta/T}}{5(1 + e^{-\delta/T})},$$

where $\delta = 0.275^\circ\text{K}$ (the magnitude of the Cr^{3+} Stark splitting). The mutual inductance is related to the magnetic temperature by

$$M = A + B/T^*.$$

The latter three equations constitute the relations used in this experiment to determine Kelvin temperature below 1.1°K . Calibration of the salt pill typically gave

$$M = 84 + 950/T^* \mu\text{H}.$$

Hence, temperature could be measured to a precision of about $(T^2/950)^\circ\text{K}$.

C. Sample Preparation

The tin sample, Sn 1-F, was cast from 99.999+% pure tin obtained from the Vulcan Detinning Company, and the indium sample, In 1-F, was cast from 99.999+% pure indium obtained from the American

Smelting and Refining Company. Both samples were cast as single crystals in graphite-coated glass tubes (1.2 mm diam) under a pressure of less than 5×10^{-6} mm Hg. After casting, the glass was etched away and the surface of the samples was cleaned with dilute hydrochloric acid. Each sample was then cut to a length of 25 mm and etched in such a way as to round the ends of the cylinder. The tin sample was further etched to a diameter of 0.9 mm. Both tin and indium were placed in glass holders and annealed for 8 h at 20°C below the melting point under a pressure of less than 5×10^{-6} mm Hg. The resistivity ratio ($R_{300^\circ\text{K}}/R_{4.2^\circ\text{K}}$) for both of these samples was greater than 18 000.

The mercury sample, Hg-10, was prepared from triply distilled, 99.999+% pure mercury obtained from Goldsmith Brothers Smelting and Refining Company. The sample holder (see insert on Fig. 1) was formed by rolling a $\frac{3}{8}$ -in.-wide strip of 0.002-in.-thick Mylar into a helix with a $\frac{3}{16}$ -in. pitch and a 0.062-in. diameter. The lower end of the helix was twisted to a point and cemented with G.E. 7031 varnish. By changing the pitch of the helix, the maximum stress the Mylar could exert on the mercury could be controlled. To facilitate further handling, the sample was placed in a brass sleeve of 0.08 in. diameter.

III. RESULTS

Details of typical transitions are shown in Fig. 2(a), 2(b), and 2(c). The amount of supercooling at 0.38°K was 14 G for tin, 15 G for indium, and 6 G for mercury. No hysteresis of the kind observed in lead was seen.¹⁵ The dashed line in Figs. 2(a) and 2(b) shows the "ideal transition" for these samples corresponding to the demagnetizing factor estimated from the length to diameter ratio. The dip in the indium transition between $\mu_e = 0.08$ and $\mu_e = 0.09$ characterized that sample during run No. 7, but was not present during earlier runs. The dip had no measurable effect on the critical

¹⁵ D. L. Decker, D. E. Mapother, and R. W. Shaw, Phys. Rev. 112, 1888 (1958).

TABLE I. Critical-field data for tin.

| H_c (G) | T (°K) | H_c (G) | T (°K) | H_c (G) | T (°K) |
|--------------|-------------|--------------|-------------|--------------|-------------|
| 303.49 | 0.3001 | 292.72 | 0.7482 | 247.91 | 1.5595 |
| 303.61 | 0.3001 | 292.68 | 0.7482 | 247.99 | 1.559 |
| 303.30 | 0.3130 | 292.10 | 0.7665 | 238.30 | 1.6818 |
| 303.00 | 0.3308 | 292.12 | 0.7665 | 238.30 | 1.6818 |
| 302.98 | 0.3308 | 291.65 | 0.7786 | 222.95 | 1.8654 |
| 302.74 | 0.3454 | 291.70 | 0.7786 | 222.87 | 1.8655 |
| 302.59 | 0.3558 | 290.61 | 0.8060 | 218.24 | 1.9180 |
| 302.24 | 0.3807 | 290.66 | 0.8060 | 218.20 | 1.9185 |
| 302.22 | 0.3807 | 289.72 | 0.8265 | 200.36 | 2.1096 |
| 301.80 | 0.4097 | 289.78 | 0.8265 | 200.37 | 2.1097 |
| 301.69 | 0.4097 | 288.88 | 0.8506 | 159.49 | 2.5022 |
| 301.21 | 0.4358 | 288.90 | 0.8506 | 159.50 | 2.5019 |
| 301.20 | 0.4358 | 287.85 | 0.8767 | 143.75 | 2.6419 |
| 300.63 | 0.4678 | 287.89 | 0.8767 | 143.64 | 2.6415 |
| 300.59 | 0.4678 | 284.99 | 0.9421 | 137.92 | 2.6906 |
| 299.97 | 0.4930 | 285.02 | 0.9421 | 137.89 | 2.6903 |
| 299.98 | 0.4930 | 282.96 | 0.9842 | 121.49 | 2.8268 |
| 298.96 | 0.5371 | 283.00 | 0.9842 | 121.38 | 2.8270 |
| 299.01 | 0.5371 | 281.26 | 1.022 | 115.18 | 2.8792 |
| 298.17 | 0.5710 | 281.27 | 1.022 | 115.11 | 2.8791 |
| 298.20 | 0.5710 | 279.06 | 1.066 | 100.53 | 2.9958 |
| 298.19 | 0.5710 | 279.03 | 1.066 | 100.53 | 2.9957 |
| 296.42 | 0.6333 | 277.63 | 1.090 | 75.36 | 3.1900 |
| 296.49 | 0.6333 | 277.64 | 1.090 | 75.39 | 3.1900 |
| 295.66 | 0.6580 | 271.92 | 1.197 | 53.94 | 3.3471 |
| 295.67 | 0.6580 | 271.99 | 1.1955 | 53.97 | 3.3471 |
| 294.79 | 0.6852 | 268.74 | 1.251 | 32.67 | 3.5020 |
| 294.84 | 0.6852 | 268.75 | 1.2488 | 32.36 | 3.5018 |
| 294.34 | 0.6997 | 264.95 | 1.311 | 32.52 | 3.5017 |
| 294.35 | 0.6997 | 265.04 | 1.3075 | 25.912 | 3.5454 |
| 293.86 | 0.7150 | 260.68 | 1.3751 | 25.899 | 3.5454 |
| 293.86 | 0.7150 | 260.67 | 1.3753 | 11.663 | 3.6441 |
| 293.32 | 0.7309 | 255.95 | 1.4459 | 11.613 | 3.645 |
| 293.24 | 0.7309 | 255.92 | 1.4459 | | |

field curve. As discussed in an earlier article,² H_c was determined by linear extrapolation of permeability curves like Fig. 2 to the field value at which $\mu_e=1$.

Experimental values of critical field and temperature are collected in Tables I, II, and III.

IV. ANALYSIS OF DATA

The entropy values to be considered here are derived from critical field data by means of the well-known thermodynamic relation,¹⁶

$$\Delta S = S_n - S_s = - (VH_c/4\pi)(dH_c/dT), \quad (1)$$

where S_n and S_s are molar entropies in the superconducting and normal state, and V is the molar volume. Comparison of experimental values has shown that entropy values derived from Eq. (1) compare favorably with results of precise calorimetric measurements.¹⁷

Given accurate values from Eq. (1), ΔS may be resolved into the individual entropy contributions from

the normal and superconducting electrons by applying the following assumptions:

- The entropies in the normal and superconducting state may be expressed as sums of independent lattice and electronic contributions (i.e., $S_n = S_{en} + S_{gn}$ and $S_s = S_{es} + S_{gs}$).
- The superconducting electronic entropy falls to zero more rapidly than the linear decrease of the normal electronic entropy as T approaches 0°K (i.e., for sufficiently low T , $S_{en} \gg S_{es}$).
- The normal electronic entropy is given by the free electron result, $S_{en}(T) = \gamma T$.
- The lattice entropy is unchanged in the superconducting transition (i.e., $S_{gn} = S_{gs}$).

These assumptions rest on a combination of experimental, theoretical, and general plausibility arguments and are usually accepted as giving an adequate description of most experimental evidence. Assumptions (a) and (c) are common to the analysis of either magnetic or calorimetric results in which context they have received frequent mention in previous work.

Assumption (d) has recently been questioned as a result of specific heat measurements on indium which

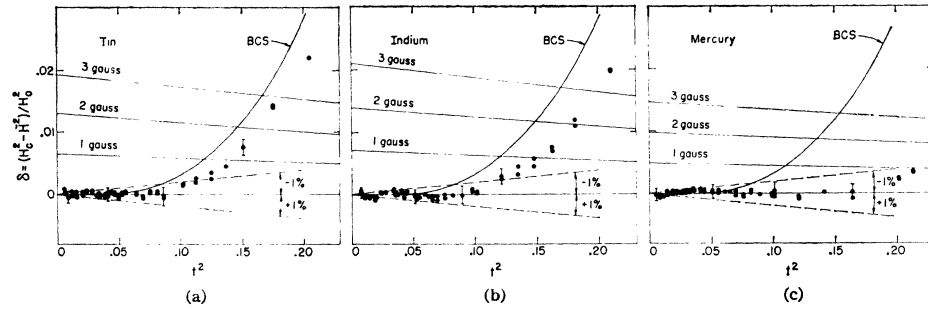
TABLE II. Critical-field data for indium.

| H_c (G) | T (°K) | H_c (G) | T (°K) | H_c (G) | T (°K) |
|--------------|-------------|--------------|-------------|--------------|-------------|
| 280.52 | 0.3001 | 268.34 | 0.7630 | 234.10 | 1.3751 |
| 280.56 | 0.3001 | 267.45 | 0.7826 | 229.13 | 1.4458 |
| 280.33 | 0.3130 | 267.43 | 0.7826 | 228.96 | 1.4459 |
| 279.16 | 0.3792 | 266.74 | 0.8022 | 220.25 | 1.5595 |
| 279.12 | 0.3792 | 266.81 | 0.8022 | 220.27 | 1.5595 |
| 278.57 | 0.4084 | 265.88 | 0.8245 | 210.00 | 1.6819 |
| 278.59 | 0.4084 | 265.74 | 0.8245 | 209.98 | 1.6818 |
| 278.07 | 0.4339 | 264.81 | 0.8479 | 193.42 | 1.8653 |
| 277.34 | 0.4653 | 264.80 | 0.8479 | 193.35 | 1.8654 |
| 277.27 | 0.4653 | 263.67 | 0.8728 | 188.47 | 1.9179 |
| 276.79 | 0.4899 | 263.61 | 0.8728 | 188.29 | 1.9177 |
| 276.80 | 0.4899 | 263.69 | 0.8728 | 169.02 | 2.1095 |
| 275.75 | 0.5349 | 262.58 | 0.8980 | 168.98 | 2.1095 |
| 275.80 | 0.5349 | 262.45 | 0.8980 | 124.46 | 2.5016 |
| 274.86 | 0.5686 | 262.53 | 0.8980 | 124.36 | 2.5023 |
| 274.86 | 0.5686 | 260.63 | 0.9391 | 107.20 | 2.6418 |
| 273.08 | 0.6309 | 260.53 | 0.9391 | 101.04 | 2.6906 |
| 273.03 | 0.6309 | 260.56 | 0.9391 | 100.98 | 2.6906 |
| 272.22 | 0.6550 | 258.36 | 0.9839 | 83.41 | 2.8271 |
| 272.19 | 0.6550 | 256.38 | 1.022 | 83.07 | 2.8270 |
| 271.36 | 0.6824 | 254.07 | 1.066 | 76.20 | 2.8794 |
| 271.32 | 0.6824 | 254.02 | 1.066 | 76.10 | 2.8792 |
| 270.76 | 0.6962 | 252.62 | 1.090 | 60.34 | 2.9956 |
| 270.79 | 0.6962 | 252.59 | 1.090 | 60.25 | 2.9956 |
| 270.18 | 0.7117 | 246.32 | 1.197 | 32.67 | 3.1899 |
| 270.29 | 0.7117 | 246.34 | 1.1955 | 32.66 | 3.1899 |
| 269.65 | 0.7279 | 242.93 | 1.251 | 10.158 | 3.3412 |
| 269.71 | 0.7279 | 242.88 | 1.2489 | 10.302 | 3.3399 |
| 269.03 | 0.7447 | 238.85 | 1.311 | 7.632 | 3.3572 |
| 268.27 | 0.7630 | 238.88 | 1.3075 | 7.600 | 3.3573 |
| | | 234.16 | 1.376 | | |

¹⁶ D. Shoenberg, *Superconductivity* (Cambridge University Press, Cambridge, England, 1952).

¹⁷ D. E. Mapother, *Phys. Rev.* **126**, 2021 (1962).

FIG. 3. Deviation of observed H_c values from $\bar{H}^2 = H_0^2 - (4\pi\gamma/v)T^2$ for (a) tin, (b) indium, and (c) mercury. The solid curve in each case gives the BCS prediction assuming $2\Delta(0) = 3.52kT_c$. Light slanting lines show loci displaced by 1, 2, and 3 G from \bar{H}^2 . Diverging dashed lines show the change in slope for $\pm 1\%$ variation in the value of γ .



have been interpreted to indicate a small increase in Debye temperature Θ_D in the superconducting transition at temperatures near 0°K .¹⁸ The significance of this apparent change in Θ_D is not clear at this writing. Since H_c data do not give a direct indication of the lattice entropy, we accept assumption (d) for the pur-

poses of the present analysis. The resulting electronic entropy results can then be studied for effects which may indicate the weakness of this assumption.

From assumptions (a) and (d) it follows that $\Delta S = S_{en} - S_{es}$ and using (c)

$$\Delta S(T) = \gamma T - S_{es}(T). \tag{2}$$

Since $\Delta S(T)$ is known from Eq. (1), it remains only to determine γ in order to solve Eq. (2) for $S_{es}(T)$.

TABLE III. Critical-field data for mercury.

| H_c (G) | T ($^\circ\text{K}$) | H_c (G) | T ($^\circ\text{K}$) | H_c (G) | T ($^\circ\text{K}$) |
|--------------|-----------------------------|--------------|-----------------------------|--------------|-----------------------------|
| 409.03 | 0.3001 | 400.09 | 0.7309 | 366.64 | 1.4454 |
| 408.98 | 0.3001 | 399.44 | 0.7482 | 366.54 | 1.4455 |
| 408.86 | 0.3130 | 399.50 | 0.7482 | 359.03 | 1.5595 |
| 408.58 | 0.3308 | 399.10 | 0.7665 | 359.06 | 1.5595 |
| 408.58 | 0.3308 | 399.08 | 0.7665 | 349.89 | 1.6818 |
| 408.41 | 0.3454 | 398.72 | 0.7786 | 349.65 | 1.6818 |
| 408.34 | 0.3454 | 398.75 | 0.7786 | 334.87 | 1.8653 |
| 408.23 | 0.3558 | 397.79 | 0.8060 | 334.82 | 1.8653 |
| 407.92 | 0.3807 | 397.07 | 0.8265 | 330.16 | 1.9180 |
| 407.92 | 0.3807 | 397.08 | 0.8265 | 330.20 | 1.9180 |
| 407.44 | 0.4097 | 396.23 | 0.8506 | 312.02 | 2.1096 |
| 407.48 | 0.4097 | 396.33 | 0.8506 | 312.00 | 2.1096 |
| 407.00 | 0.4358 | 395.23 | 0.8767 | 268.39 | 2.5014 |
| 406.93 | 0.4358 | 395.28 | 0.8767 | 268.61 | 2.5014 |
| 406.40 | 0.4678 | 392.82 | 0.9421 | 251.33 | 2.6414 |
| 406.45 | 0.4678 | 392.81 | 0.9421 | 251.39 | 2.6415 |
| 406.05 | 0.4930 | 391.12 | 0.9842 | 244.95 | 2.6902 |
| 405.96 | 0.4930 | 391.04 | 0.9842 | 244.98 | 2.6908 |
| 405.06 | 0.5371 | 389.56 | 1.022 | 226.35 | 2.8273 |
| 405.07 | 0.5371 | 387.59 | 1.066 | 226.37 | 2.8269 |
| 404.30 | 0.5710 | 387.61 | 1.066 | 219.41 | 2.8786 |
| 404.37 | 0.5710 | 386.38 | 1.090 | 219.30 | 2.8789 |
| 402.82 | 0.6333 | 386.35 | 1.090 | 202.55 | 2.9946 |
| 402.85 | 0.6333 | 383.30 | 1.154 | 173.30 | 3.1896 |
| 402.17 | 0.6580 | 383.32 | 1.154 | 173.34 | 3.1897 |
| 401.42 | 0.6852 | 381.27 | 1.197 | 122.03 | 3.5018 |
| 401.47 | 0.6852 | 381.38 | 1.193 | 122.45 | 3.5000 |
| 401.05 | 0.6997 | 378.33 | 1.251 | 84.51 | 3.7142 |
| 401.10 | 0.6997 | 378.38 | 1.249 | 84.45 | 3.7156 |
| 400.64 | 0.7150 | 374.94 | 1.311 | 11.694 | 4.0956 |
| 400.63 | 0.7150 | 375.06 | 1.3075 | 11.694 | 4.0956 |
| 400.12 | 0.7309 | 370.99 | 1.3760 | 3.461 | 4.1366 |
| 400.08 | 0.7309 | 371.05 | 1.3759 | 3.550 | 4.1363 |
| | | 371.07 | 1.3751 | | |

(A). Determination of γ

From Eq. (2) and assumption (d) it is clear that $\lim_{T \rightarrow 0} \kappa \Delta S(T) = \gamma T$. As recently emphasized by Swenson,¹⁹ the implication of this behavior in terms of $H_c(T)$ is that

$$H_c^2 = H_0^2 - (4\pi\gamma/V)T^2, \tag{3}$$

where the constant H_0 is the intercept of the critical field curve at 0°K . From Eq. (3), we expect a linear relation between the *squares* of the coordinates of the critical field at sufficiently low temperatures. With increasing T , nonlinear contributions to $\Delta S(T)$ (from S_{es}) produce a slight curvature or bend in an experimental plot of H_c^2 versus T^2 . The experimental demonstration of such a characteristic in this plot is evidence that the measuring temperatures are small enough to reach the limiting region where $\Delta S(T)$ is linear and (under the present assumptions) solely due to the normal electronic entropy. The slope of the H_c^2 versus T^2 plot below the bend permits determination of γ .

Experimentally, the bend in H_c^2 versus T^2 is slight; very precise H_c data are required to resolve it. In order to show its existence clearly on a graph, we plot the quantity

$$\delta = (H_c^2 - \bar{H}^2)/H_0^2,$$

where

$$\bar{H}^2 = H_0^2 - (4\pi\gamma/V)T^2. \tag{4}$$

The \bar{H}^2 defined by Eq. (4) is the straight line on a plot of H_c^2 versus T^2 which gives the best fit to the linear portion of the experimental curve at temperatures below the bend. Thus, δ presents the deviation of the experimental H_c curve from the limiting linear behavior

¹⁸ C. A. Bryant and P. H. Keesom, Phys. Rev. Letters 4, 460 (1960); C. A. Bryant and P. H. Keesom, Phys. Rev. 123, 491 (1961); and H. R. O'Neal and N. E. Phillips, *ibid.* 137, A748 (1965).

¹⁹ J. E. Schirber and C. A. Swenson, Phys. Rev. 123, 1115 (1961).

TABLE IV. Superconducting- and normal-state parameters.

| Sample | H_0^a (G) | T_c^a (°K) | γ^a (mJ/mole °K) | T_c/Θ_D | V (cc/mole) | $2\Delta(0)/kT_c^b$ | K |
|--------|-----------------|-------------------|----------------------------|----------------|---------------------|---------------------|-------|
| Sn1-F | 305.50 ±0.10 | 3.7216 ±0.0010 | 1.744 ±0.010 | 0.019 | 16.064 ^c | 3.60 ±0.02 | 1.012 |
| In1-F | 282.66 ±0.12 | 3.4070 ±0.0010 | 1.659 ±0.012 | 0.031 | 15.37 ^d | 3.64 ±0.02 | 0.985 |
| Hg-10 | 410.88 ±0.12 | 4.1540 ±0.0010 | 1.809 ±0.012 | 0.052 | 13.79 ^e | 3.96 ±0.02 | 0.835 |

^a These values supersede earlier reported values. See Ref. 20.

^b $2\Delta(0)$ is obtained from Eq. (5). Errors reflect only the uncertainty in H_0 , γ , and V .

^c J. A. Rayne and B. S. Chandrasekhar, Phys. Rev. **120**, 1658 (1960).

^d C. A. Swenson, Phys. Rev. **100**, 1607 (1955).

^e See Ref. 19.

described by Eq. (3). For convenience in comparisons between different superconducting elements, δ is expressed in reduced units of H_0 and is plotted versus the square of the reduced temperature, $t = (T/T_c)$. It will be recognized that since this method of presentation involves the subtraction of analytic functions from the experimental values, the relative scatter in the data is considerably magnified.

Plots of experimental data for Sn, In, and Hg are shown in Figs. 3(a), 3(b), and 3(c). The solid curves on these figures show the form of δ predicted by the BCS theory for an energy gap of $3.52kT_c$. For each of the three elements, the experimental points scatter about $\delta=0$ on the left-hand side of the figure and rise steeply for sufficiently large temperature. The upturn in the trend of the δ values corresponds to the bend in the H_c^2 -versus- T^2 data and represents the onset of the contribution of S_{es} . Values of γ for each element are determined from the coefficient of T^2 in Eq. (4) which is fitted by least squares to the H_c data for temperatures below the bend. Numerical values of γ and H_0 determined from Eq. (4) are collected in Table IV. These values supersede earlier published results²⁰ in which γ

and H_0 were estimated by parabolic extrapolation for H_c data from above 1°K. Agreement with the earlier data is satisfactory in the temperature range where the measurements overlap.

The small undulations which appear in the low-temperature linear region are ignored since the amplitude is about equal to the experimental limit of precision (see representative error bars in figures). The two diverging lines immediately above and below the axis, $\delta=0$, correspond to slopes differing by $\pm 1\%$ from the best fit to the low-temperature data.

An indication of the actual magnitude of the low-temperature bend in the critical field curve is provided by the slanted lines in Figs. 3(a), 3(b), and 3(c). Each slanted line gives a locus of constant deviation in magnetic field with respect to \bar{H} . Thus, for example, the line labeled "1 gauss" corresponds to a curve parallel to the low-temperature limiting critical field curve and displaced from it by 1 G. Since the H_c values can be determined experimentally with an absolute precision of the order of 0.1 G, the bend is resolvable without difficulty.

(B). Calculation of the Energy Gap

There are several ways in which the measured thermodynamic properties of the present work can be related to the electronic gap, $2\Delta(T)$, of the BCS theory.²¹ The theory relates H_0 and γ to the energy gap by the equation

$$\Delta(0) = H_0(\pi k^2 V / 6\gamma)^{1/2}, \quad (5)$$

where $2\Delta(0)$ is the energy gap at 0°K and k is Boltzmann's constant. Moreover, the complete temperature dependence of H_c and S_{es} has been derived from the BCS theory by Mühlischlegel.²²

$$H_c^2 / 8\pi\gamma T_c^2 = \frac{3}{2}(xa' - a)t^2, \quad (6)$$

$$S_{es} / \gamma T_c = t[1 + 3(xa' - a) - 3x/2], \quad (7)$$

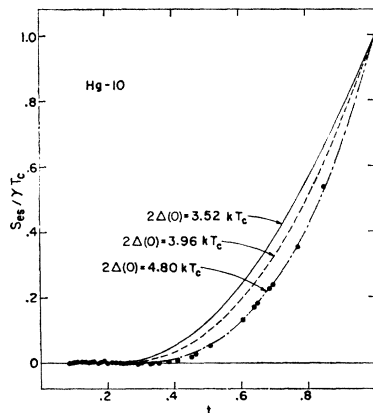


FIG. 4. Superconducting electronic entropy for mercury. Solid and dashed curves show calculated results obtained by scaling the BCS theory using $\Delta(t) = \alpha\Delta_{\text{BCS}}(t)$.

²⁰ D. K. Finnemore, D. E. Mapother, and R. W. Shaw, Phys. Rev. **118**, 127 (1960); and R. W. Shaw, D. E. Mapother, and D. C. Hopkins, *ibid.* **120**, 88 (1960).

²¹ J. Bardeen, L. N. Cooper, and J. R. Schrieffer, Phys. Rev. **108**, 1175 (1957).

²² B. Mühlischlegel, Z. Physik **155**, 313 (1959).

where

$$x = (\Delta(T)/\pi kT)^2,$$

$2\Delta(T)$ = energy gap at temperature T ,

$$a = -\frac{2}{\pi} \int_{-\infty}^{\infty} \ln\{1 + \exp[-\pi(u^2 + x)^{1/2}]\} du$$

$$+ x\{\ln(1.781x^{1/2}) - \frac{1}{2}\} + \frac{1}{3},$$

and

$$a' = da/dx.$$

The solid lines shown in Figs. 3(a), 3(b), and 3(c) were derived from Eq. (6) using the original BCS value of $2\Delta(0) = 3.52kT_c$. These figures show that, taken literally, the BCS theory deviates from the experimental results in two respects: (1) None of these elements show the value $2\Delta(0) = 3.52kT_c$, and (2) the simplifying assumptions of the theory predict that all superconducting elements should show the same relative energy gap function. In order to give a more specific idea of the revisions in the theory necessary to improve agreement with experiment, we shall assume the validity of the BCS formulas, Eqs. (5), (6), and (7), and see what adjustments in $\Delta(T)$ are required to fit the present results.

The first adjustment procedure was to scale the BCS temperature-dependent energy gap by a constant multiplier, α , [i.e., $\Delta(t) = \alpha\Delta_{BCS}(t)$] and seek values of $\Delta(0)$ which give the best fit to the experimental data. Figure 4 gives three calculated curves which show (in reduced units) the effect on the temperature dependence of S_{es} of scaling $\Delta(0)$. The points on the $4.80kT_c$ curve correspond to the experimental data for Hg. The corresponding effect on H_c is presented in terms of the deviation function, $D(t)$ in Fig. 5. For comparable changes in $\Delta(0)$, the shape of $D(t)$ is considerably more sensitive than S_{es} , and it is also more easily derived from critical field measurements.¹⁷

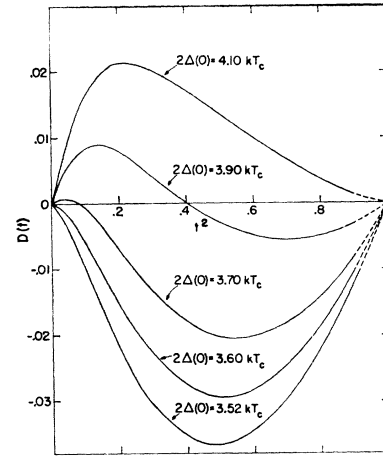


FIG. 5. Variation of calculated deviation function with energy-gap scaling factor.

Figures 6(a) and 6(b) show the comparison between theoretical curves and experimental values of S_{es} for Sn and In. The theoretical curves were calculated using $\Delta(0)$ values given by Eq. (5) for each element. The experimental points are computed from Eq. (2) using the γ values determined as described in the preceding section. The agreement is fairly good for Sn and In, but the much larger value, $2\Delta(0) = 4.80kT_c$, is required to give a satisfactory fit for Hg (see Fig. 6).

In Fig. 7 experimental values of $D(t)$ for Sn, In, and Hg are compared with curves calculated from Eq. (6), again using $\Delta(0)$ values determined from Eq. (5). The agreement is satisfactory only at the lowest temperatures, although it can be improved somewhat at higher t by using larger values of $\Delta(0)$. As in the entropy curves [Figs. 4 and 6(a) and 6(b)], the discrepancy is greatest for Hg.

The foregoing attempts to fit H_c and S_{es} have accepted the original BCS form of $\Delta(t)$ and used $\Delta(0)$ as the only adjustable parameter. It is, of course, possible to invert the procedure and use Eqs. (5) and (6) to

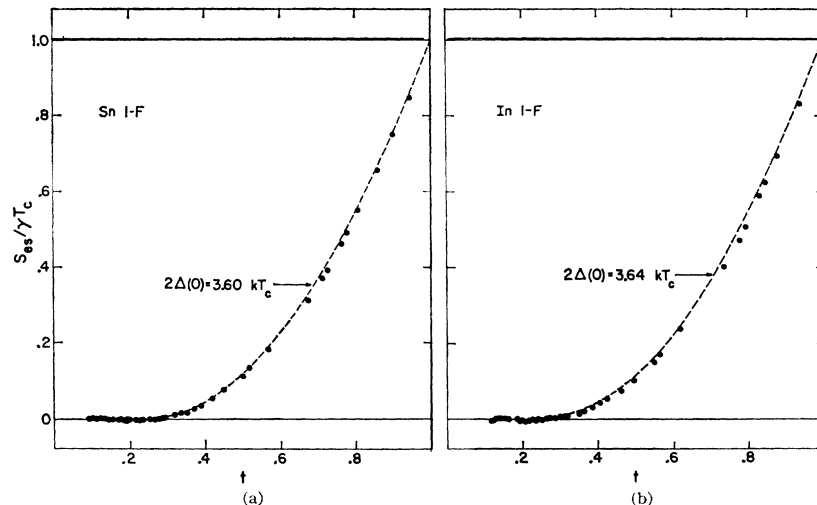


FIG. 6. Superconducting electronic entropy for (a) tin, and (b) indium. Dashed curves show S_{es} obtained from the BCS theory using scaled values of the energy gap as noted.

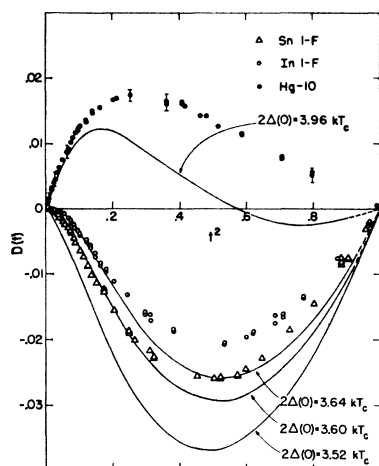


FIG. 7. Comparison of experimental deviation functions with curves calculated by scaling the energy gap.

determine $\Delta(t)$ from the observed H_c . Figure 8 shows values of $\Delta(t)/\Delta(0)$ computed in this way for Sn, In, and Hg. It is evident that rather minor modifications in the temperature dependence of Δ would suffice to give agreement with the observed H_c data.

V. DISCUSSION

(A). Energy-Gap Results

In Table V the values of $\Delta(0)$ deduced from the present measurements are compared with corresponding values from direct energy-gap measurements by infrared and tunneling experiments. Generally, the agreement seems remarkably good.

The present semiempirical application of the BCS theory yields different values of $\Delta(0)$, depending on

TABLE V. Various determinations of $2\Delta(0)/kT_c$.

| Method of determination | Tin | Indium | Mercury |
|--|--------------------|--------------------|--------------------|
| $\Delta(0) = H_0[\pi k^2 V / 6\gamma]^{1/2}$ | 3.60 ± 0.02 | 3.64 ± 0.02 | 3.96 ± 0.02 |
| Shape of $S_{ee}/\gamma T_c$ -versus- t curve ^a | 3.63 | 3.68 | 4.8 |
| Infrared absorption in bulk samples ^b | 3.6 ± 0.2 | 4.1 ± 0.2 | 4.6 ± 0.2 |
| Infrared absorption in thin films ^c | 3.3 ± 0.2 | 3.9 ± 0.3 | |
| Electron tunneling ^{d-e} | 3.46 ± 0.10 | 3.64 ± 0.10 | 4.60 ± 0.11 |
| Calorimetric ^{a,b} | 3.44 | 3.26-3.77 | 3.96 |

^a This derivation of $2\Delta(0)/kT_c$ is most sensitive to the high-temperature behavior of the data.

^b P. L. Richards and M. Tinkham, Phys. Rev. 119, 575 (1960).

^c D. M. Ginsberg and M. Tinkham, Phys. Rev. 118, 990 (1960).

^d Ivar Giaever and Karl Meierle, Phys. Rev. 122, 1101 (1961).

^e I. Giaever, H. R. Hart, and K. Meierle, Phys. Rev. 126, 941 (1962).

^f Stuart Berman and D. M. Ginsberg, Phys. Rev. 135, A1356 (1964).

^g See Ref. 18.

^h See Ref. 25.

whether one fits the limiting experimental results as the temperature approaches zero, or, instead, seeks the best average fit over the whole superconducting temperature range. As suggested by the results of Fig. 8, these differences probably result from inaccuracy in the temperature dependence of the BCS $\Delta(t)$ at the higher t values. In order to fit the S_{ee} results, abnormally large values of $\Delta(0)$ are required to make $\Delta(t)$ rise more rapidly than the BCS function. The difference is most pronounced for Hg, a "strong-coupling" superconductor, for which the simplifying assumptions of the BCS theory are probably not valid.²¹ It is known experimentally that deviations from the BCS law of corresponding states correlate with the ratio, T_c/Θ_D .²³ (Values of T_c/Θ_D are given in Table IV.) Discussions of the theoretical implications of these H_c data for the energy-gap function have recently been given by various authors.²⁴

The differences between the low- and high-temperature values of $\Delta(0)$ in the cases of Sn and In, while qualitatively similar to the behavior of Hg, are much smaller than the spread in values reported from direct measurements of $\Delta(0)$. For Hg, however, the difference is substantial. It is noteworthy that the infrared and tunneling data are in much better agreement with the H_c energy gap which gives greatest weight to the high-temperature data.

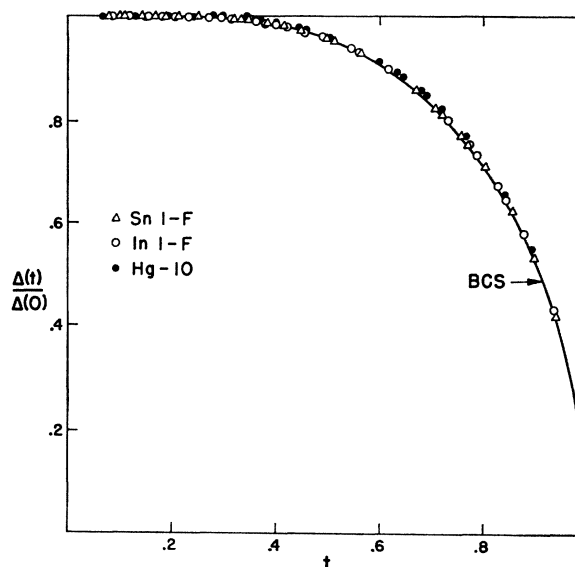


FIG. 8. Temperature dependence of the energy gap as computed from H_c data using Eq. (6).

²³ J. Bardeen and J. R. Schrieffer, *Progress in Low Temperature Physics* (North-Holland Publishing Company, Amsterdam, 1961), Vol. III.

²⁴ J. C. Swihart, Phys. Rev. 131, 73 (1963); Y. Wada, Phys. Rev. 135, A1481 (1964); D. J. Scalapino, Y. Wada, and J. C. Swihart, Phys. Rev. Letters 14, 102 (1965); J. C. Swihart, D. J. Scalapino, and Y. Wada, *ibid.* 14, 106 (1965); and John Bardeen and Michael Stephen, Phys. Rev. 136, A1485 (1964).

TABLE VI. Comparison with related measurements.

| | T_c °K | H_0 (G) | γ mJ/mdeg ² | α_n (mJ/mole deg ⁴) | α_s |
|---|-------------|--------------|----------------------------------|---|------------|
| Tin | | | | | |
| This work | 3.722 | 305.50 | 1.74 | | |
| Bryant and Keesom ^a | 3.701 | 306 | 1.80 | 0.242 | 0.242 |
| O'Neal and Phillips ^b | | | 1.78 | 0.246 | 0.246 |
| Rayne and Chandrasekhar ^c | | | | 0.238 | 0.238 |
| Corak and Satterthwaite ^d | 3.722 | 303.4 | 1.74 | | |
| Indium | | | | | |
| This work | 3.407 | 282.66 | 1.66 | | |
| Bryant and Keesom | 3.403 | 284 | (I) 1.61 (II) 1.59 | 1.50 1.53 | ~1.1 |
| O'Neal and Phillips | | 285 | 1.69 | 1.42 | 1.22 |
| Rayne and Chandrasekhar ^e | | | | 1.41 | 1.41 |
| Mercury | | | | | |
| This work | 4.154 | 410.88 | 1.81 | | |
| Phillips, Lambert, and Gardner ^f | | | 1.86 | 5.20 | 5.20 |
| van der Hoeven and Keesom ^g | 4.16 | 380±60 | 1.79 | 5.23 | 5.23 |

^a See Ref. 18.^b See Ref. 24.^c J. A. Rayne and B. S. Chandrasekhar, Phys. Rev. **120**, 1658 (1960).^d W. S. Corak and C. B. Satterthwaite, Phys. Rev. **102**, 662 (1956).^e See Ref. 26.^f N. E. Phillips, M. H. Lambert, and W. R. Gardner, Rev. Mod. Phys. **36**, 131 (1964).^g See Ref. 25.

Values of $\Delta(0)$ listed in the last line of Table V have been derived from calorimetric measurements by fitting the low-temperature values to the approximate expression, $C_{es}(t) = a \exp(-bt^{-1})$. They are listed here for completeness and to show that no major discrepancies exist. However, because of the difference in the nature of the measurement and the mode of analysis, the calorimetric values of $\Delta(0)$ cannot be compared with our magnetically derived values without going into several questions of interpretation which are not directly pertinent to the present measurements. For this reason we prefer to give this comparison in a separate article.

(B). Normal Electronic Specific Heat

Table VI compares the present γ values with recent calorimetric data which extend below 1°K. Since the calorimetric values are derived from measurements of the total heat capacity C_n , we also include values of α , the coefficient of the T^3 term in C_n from which the limiting value of the Debye temperature is obtained. While the agreement between the magnetic and calorimetric values of γ is reasonably good, the differences are larger than our estimated error of 0.7%.

Bryant and Keesom have reported anomalous behavior in the lattice specific heat of In.¹⁸ Below about 0.8°K, the total measured heat capacity C_s falls below the lattice contribution alone as determined from C_n . Expressed in terms of the limiting value of the Debye temperature, the observed effect is equivalent to a 9% increase of Θ_D in the superconducting state. Qualitative substantiation of these results has been found in recent measurements of O'Neal and Phillips, although the

magnitude of the apparent shift in Θ_D is about half as large.¹⁸ Both Bryant and Keesom, and O'Neal and Phillips, find no corresponding effect in similar measurements on Sn nor do the recent measurements of van der Hoeven and Keesom²⁵ show such an effect in Hg.

The inferred change in lattice specific heat of In, if correct, invalidates assumption (d) of the present analysis. In addition to the electronic entropy difference, $(S_{en} - S_{es})$, the ΔS values derived from critical-field data should contain a contribution from the difference in lattice entropies if such a difference is present. In fact, the quantity we have identified as S_{es} would instead be $(S_{es} - \Delta S_\theta)$, where ΔS_θ is the difference in lattice entropies. According to Bryant and Keesom, ΔS_θ is a positive quantity which increases as T^3 .

Plots of our ΔS -versus- T data are shown in Fig. 9 for $T < 1^\circ\text{K}$. For In, like Sn and Hg, the limiting temperature dependence of ΔS seems accurately linear within our experimental accuracy. All of the ΔS -versus- T curves extrapolate linearly to the origin as required by the third law of thermodynamics. In other words, all of our results, including those for In, show the behavior expected if ΔS were due solely to the difference in electronic entropies.

It should be recognized that the Bryant and Keesom anomaly is quite a small effect. Moreover, knowledge of its temperature dependence is limited to the observation that it apparently varies as T^3 at the lowest temperatures. If, for purposes of estimation, we assume that the lattice contribution to ΔS varies as T^3 , it is

²⁵ B. J. C. van der Hoeven, Jr. and P. H. Keesom, Phys. Rev. **135**, A631 (1964).

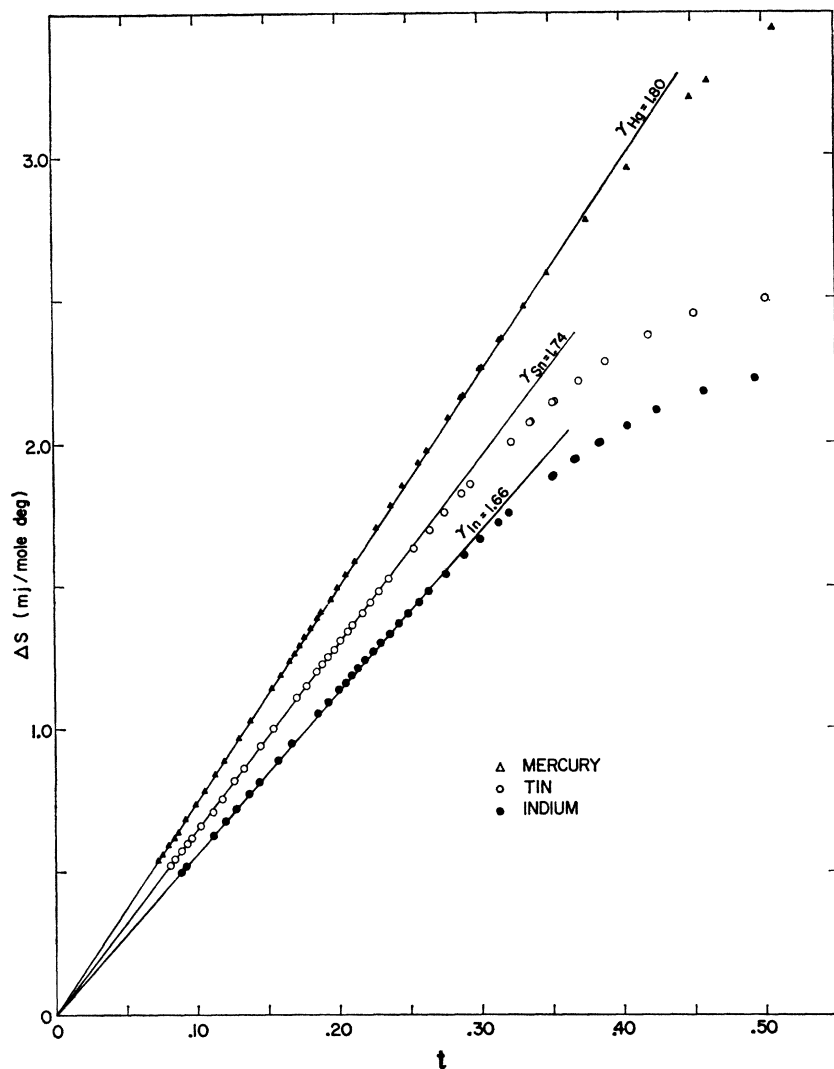


FIG. 9. Entropy difference, $\Delta S = S_n - S_s$, versus t showing limiting behavior as $T \rightarrow 0^\circ\text{K}$.

easily shown that $\Delta S_\theta/\gamma T \approx (\Delta\alpha/3)T^2$. Using Bryant and Keesom's value for $\Delta\alpha = (\alpha_n - \alpha_s)$, the deviation of ΔS from the linear γT dependence is $< 1\%$ at 0.3°K , $\sim 2\%$ at 0.5°K , $\sim 4\%$ at 0.7°K , and $\sim 8\%$ at 1°K . With present accuracy, our data cannot rule out the occurrence of such a small anomaly below 0.5°K . However, it would give an appreciable contribution above 0.7°K which would drastically alter the temperature dependence of S_{es} from that deduced in the present analysis. [Referring to Fig. 6(b), note that under the assumptions of the present thermodynamic analysis S_{es} for In does not become as large as $0.1\gamma T_c$ until $t \approx 0.5$ or 1.7°K .] Thus, the fact that our derived S_{es} for In shows the expected close similarity to S_{es} for Sn (which is not anomalous) makes the existence of a ΔS_θ term of this magnitude seem quite improbable above 0.7°K .

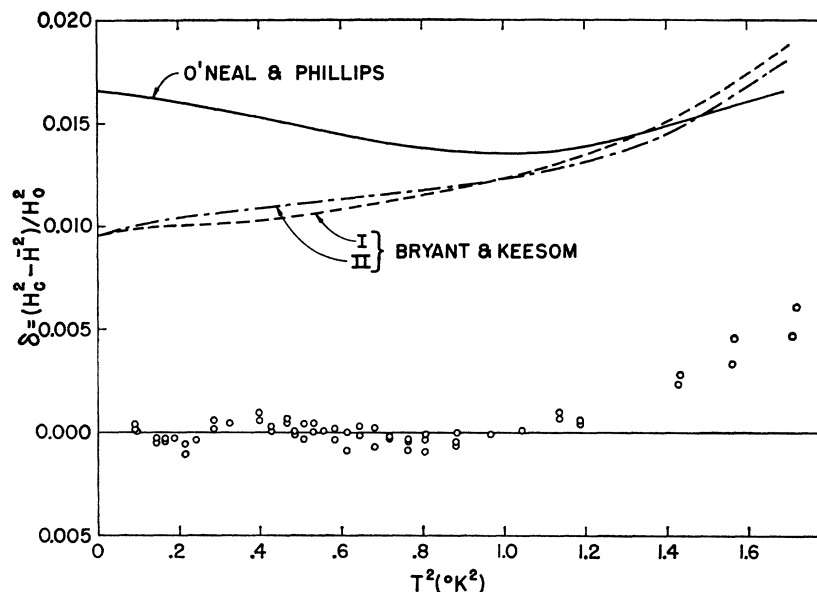
Because of the impossibility of unambiguously separating S_{es} and ΔS_θ in the present analysis, it is at least conceivable that $(S_{es} - \Delta S_\theta)$ might fortuitously have

the same temperature dependence as S_{es} for Sn. But, if this were true, the present results for $\Delta(t)$ of In would require revision whereas, in fact, they seem to be in satisfactory accord with direct measurements of the energy gap by methods which are insensitive to the lattice entropy.

In this connection it may also be noted that Chandrasekhar and Rayne have looked for the lattice anomaly in In by acoustical measurement of Θ_D in the normal and superconducting states.²⁶ Within the accuracy of their experiment (1%) there was no detectable difference in Θ_D between the superconducting and normal states. Since the determination of Θ_D from measurements of the velocity of sound involves some assumptions, the difference between acoustic and calorimetric results does not necessarily indicate errors in either experiment. However, it is interesting to note

²⁶ B. S. Chandrasekhar and J. A. Rayne, Phys. Rev. **124**, 1011 (1961).

FIG. 10. Comparison of observed values of H_c with results derived from calorimetric measurements on indium. Points give the same data shown in Fig. 3(b). Solid curves show corresponding results calculated from analytic expressions used by O'Neal and Phillips (Ref. 18) and Bryant and Keesom (Ref. 18) to fit their specific heat data.



that if the Bryant and Keesom data for In are fitted using the Θ_D value determined by Chandrasekhar and Rayne, the resulting γ value is 1.65 mJ/mole deg², in good agreement with the present results.

The disagreement between the present measurements and the calorimetric data of Bryant and Keesom and O'Neal and Phillips is shown most directly on Fig. 10. Here, the same data of Fig. 3(b) are shown together with the corresponding curves for δ computed from the analytical expressions used by the calorimetric workers to describe their experimental results. The calorimetrically deduced curves lie well beyond the likely experimental error of the magnetic data. Most of the difference in Fig. 10 is due to the fact that the expressions used to fit the calorimetric data give an appreciably larger value of H_0 than is observed in direct measurement. The thermodynamic relations used to calculate H_0 from specific heat data require integration of $\Delta C(T)$ over the whole superconducting temperature range. Thus, the difference in the H_0 values indicates that the *average* values of $\Delta C(T)$, (as determined from the expressions used to fit the calorimetric data) are about 1% too large. This is within the expected range of accuracy for the measurements under consideration. However, it will also be noted that the slopes of the calorimetric curves of Fig. 10 differ from the horizontal asymptote of the magnetic data. This occurs because the calorimetric investigators assign different values of γ to fit their observations of C_n below 1°K. As also shown in Table VI, the two calorimetric groups report γ values for In which lie above or below our magnetically deduced value by about the same amount. In other words, our value of γ roughly averages the values reported from the separate calorimetric measurements. Further analysis of the experimental significance

of the disparity in γ values is in progress and will be reported later.

APPENDIX A: LOW-TEMPERATURE BEHAVIOR OF $D(t)$

Both Bryant and Keesom and O'Neal and Phillips¹⁸ have called attention to the fact that the deviation function $D(t)$, computed from their calorimetric data, changes sign at the lowest temperatures. O'Neal and Phillips assert that their positive values of $D(t)$ "are a direct consequence" of the presumed lattice anomaly in In. We doubt the uniqueness of this interpretation. It can be shown that such behavior may also be interpreted as simply another manifestation of the well established and systematic pattern of deviation shown by superconducting elements from the law of corresponding states predicted by the original BCS theory.

We define

$$D(t) = h - (1 - t^2),$$

and from Eq. (3)

$$h = \frac{H_c}{H_0} = \left[1 - \frac{4\pi\gamma T_c}{V H_0} t^2 \right]^{1/2}. \quad (8)$$

For brevity, let

$$K = (2\pi\gamma/V)(T_c/H_0)^2, \quad (9)$$

where K is a characteristic constant of the superconducting material. For small t values where Eq. (3) is valid,

$$D(t) = (1 - K)t^2 - \frac{K^2}{2}t^4 - \frac{K^3}{2}t^6. \quad (10)$$

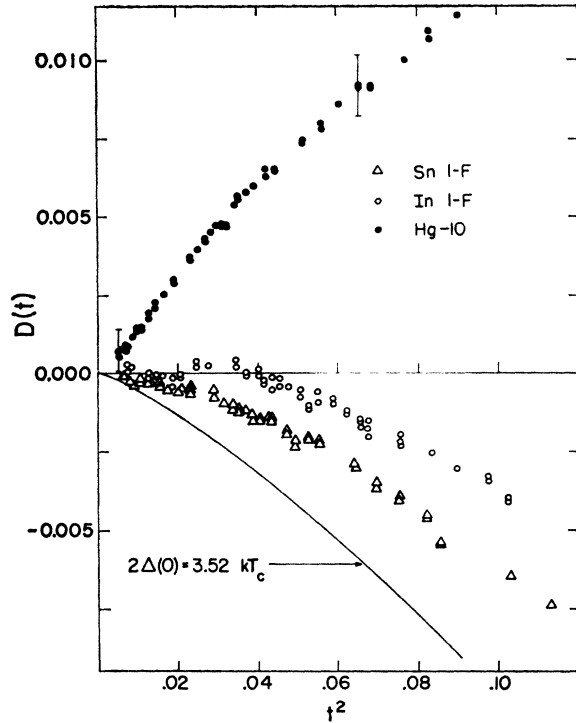


FIG. 11. Experimental values of the deviation function for tin, indium, and mercury near 0°K. The calculated result from the BCS theory is shown by the solid curve.

From Eq. (10) it is clear that K determines the slope of $D(t)$ near $t=0$. If $K < 1$, then the slope is initially positive, and if $K > 1$, then the slope is initially negative.

The substitution of Eq. (5) into Eq. (9) reveals that K is also a measure of the ratio of energy gap to critical temperature,

$$K = [(3.63kT_c)/(2\Delta(0))]^2.$$

According to this result, the initial slope of $D(t)$ will

change sign at $2\Delta(0) = 3.63kT_c$, or very close to the value obtained for In. (Figure 5 shows this behavior graphically.)

A tabulation of K for tin, indium, and mercury is given in Table IV. If K is substantially less than unity (as for Hg), $D(t)$ can be positive over the entire range, $0 < t < 1$. For In, the $D(t)$ derived from our magnetic data shows a positive maximum of 1.1×10^{-4} at $t^2 = 0.015$ corresponding in absolute units to a deviation of 0.03 G at 0.416°K. This is below the limit of resolution of the present measurements. The actual experimental points for $D(t)$ near 0°K are shown in Fig. 11.

These considerations suggest that $D(t)$ should be used with caution near 0°K. The reason for the pronounced curvature in $D(t)$, which is still evident for $t^2 < 0.1$, is simply that the critical-field curve deviates appreciably from a T^2 temperature dependence in this range. For the purpose of determining γ , $D(t)$ is distinctly inferior to the use of Eq. (3). While the validity of Eq. (3) has been recognized for a long time, it has often been assumed that its ultimate convergence to a parabolic temperature dependence near 0°K justified the determination of γ from the slope of an experimental plot of H_c versus T^2 . The present data show that the temperature below which an H_c versus T^2 plot finally straightens out may be somewhere below $t^2 = 0.02$, depending on the value of K . Since no previous H_c measurements have been extended to such a low t , this probably accounts for the poor reputation for accuracy that magnetically determined γ values have enjoyed in the past. On the other hand, the H_c^2 versus T^2 curve straightens out as soon as the S_{e2} contribution becomes negligible. This occurs at about $t = 0.28$ for Sn and at $t = 0.35$ for Hg owing to its larger $\Delta(0)$. Thus, the H_c^2 versus T^2 plot gives the experimenter a larger and more useful T range over which to determine the slope which fixes γ .